Structural Engineering and Mechanics, Vol. 15, No. 3 (2003) 367-378
DOI: http://dx.doi.org/10.12989/sem.2003.15.3.367

A study on the measurement of plastic zone and crack growth length at the crack tip under cyclic loading using ESPI system

Kyung-Su Kim†, Ki-Sung Kim† and Chun-Sik Shim‡

Department of Naval Architecture and Ocean Engineering, Inha University, Incheon 402-751, Korea

(Received August 16, 2002, Accepted February 28, 2003)

Abstract. The magnitude of the plastic zone around the crack tip of DENT (Double Edge Notched Tension) specimen and the crack growth length under cyclic loading were measured by ESPI (Electronic Speckle Pattern Interferometry) system. The measured magnitude of plastic zone was compared with the proposed by Irwin and calculated by a nonlinear static method of MSC/NASTRAN. The measured crack growth length by ESPI system was also compared with the obtained data by the image analysis system. From the study, it is confirmed that the plastic zone and crack growth length can be measured accurately with the high-tech equipment (ESPI System).

Key words: electronic speckle pattern interferometry system; plastic zone size; strain distribution; crack growth length; crack growth rate.

1. Introduction

A few techniques for plastic zone measurement are known by now. However, a satisfactory, generally applicable technique is still not available. Among existing techniques, the microhardness technique is applicable to materials that strongly work harden (like austenitic stainless steels). The procedure is simply taking hardness indentations ahead or around the crack tip and determining the elastic-plastic boundary as a sudden variation in hardness. In the foil strain gauge technique, a tiny strain gauge is located on the specimen so that it is parallel to the loading direction ahead of the crack tip. During loading, the output from the strain gauge is recorded as a stress-strain diagram. When strain becomes nonlinear, the distance from the crack tip to the strain center is determined as the plastic zone size. Electronic speckle pattern technique is used in optical metrology, particularly in the measurement of deformations and displacements. When compared to a standard method such as strain gauges, the advantage of this technique is that the displacements at all points on a surface, rather than a selected point only, is recorded simultaneously.

When the load is applied in the structural material, theoretical infinite stresses at the tip of sharp crack would not appear in real structural materials because a crack tip becomes blunted and a region

† Professor
‡ Doctor

of yielding, crazing, or microcracking forms. It is significant that the region of yielding, called the plastic zone, must be finite. This is simply the distance ahead of the crack tip where the elastic stress distribution exceeds the yield criterion. Due to yielding within the plastic zone, the stresses are lower than the values from the elastic stress field equations. The yielded material thus offers less resistance than expected one, and large deformation occurs. It gives significant influence on the fatigue crack growth rate and consequently on fatigue life.

For many fatigue-critical parts of ships and offshore structures, fatigue crack propagation under service conditions generally involves random or variable loading, rather than constant amplitude loading. Significant acceleration and/or retardation in crack growth rate can occur as a result of these load variations. Thus, an accurate prediction of fatigue life requires an adequate evaluation of these load interaction effects. However, the previous studies on the retardation due to overloading in the fatigue crack growth behavior were not satisfactory due to the lack of accurate test data of plastic zone size which affects the retardation factor. For a given material and set of test conditions, the fatigue crack can be described by the relationship between cyclic crack growth rate da/dN and stress intensity range ΔK (Dowling 1993). This stress intensity range depends on the crack growth length and especially cyclic crack growth rate depends on the plastic zone size at the retardation due to overloading. The traditional fatigue crack growth equations which consider the plastic zone sizes are based on simple assumptions and do not consider real complexities of structures. Therefore it is very important to measure the real values of the plastic zone size at the crack tip and crack growth length to analyze accurately the behavior of crack growth under the cyclic loading.

In this paper, therefore, the plastic zone size at the crack tip of DENT (Double Edge Notch Tension) specimen under constant-amplitude cyclic loading and the fatigue crack growth length were examined by ESPI system. With this ESPI system, it is possible to measure the strain distribution on the whole measuring area including critical points. Comparisons are made between these experimental results and the results of the plastic zone size calculated by Irwin's estimate and MSC/NASTRAN. Also the crack growth length was measured by ESPI system and image analysis system.

2. Principle of ESPI system

ESPI (electronic speckle pattern interferometry) system allows for non-contact whole-field measurement of the surface displacements. The surface of the specimen is illuminated with the laser from ESPI system. The scattered light is captured by CCD (charge-coupled device) camera, and the image is stored in computer memory. This is done twice, before and after the specimen is deformed. The two images are then subtracted and displayed on a video monitor. The resulting image exhibits subtraction correlation fringes whose shape and spacing depend on the magnitude and direction of the surface's movement and on the geometry of the optical setup. The detailed pattern of strain development over the surface of the specimen can then be analyzed (Gong and Toyooka 1999).

Fig. 1 depicts a simple illumination arrangement sensitive to in-plane displacements in one direction. A plane object is illuminated with two coherent collimated and coplanar light beams that make angles θ_1 and θ_2 with respect to the object's surface. The diffusely reflected light is captured by CCD camera, whose line of sight is perpendicular to the surface. The intensity that reaches the camera's sensor is (Jones and Wykes 1989)

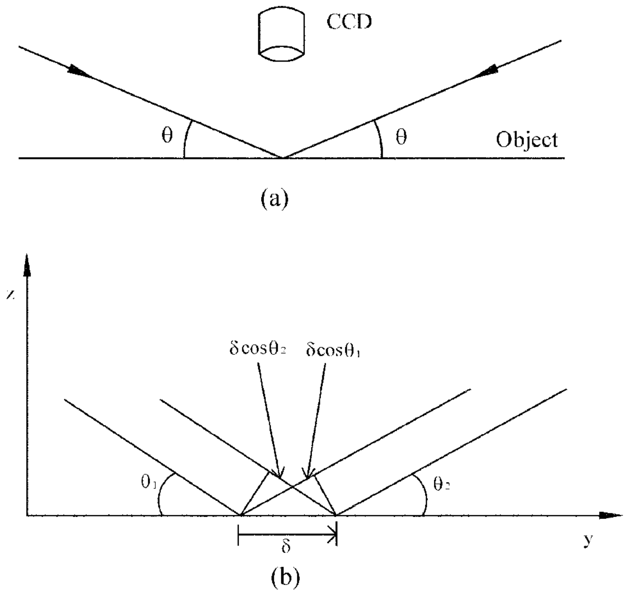

Fig. 1 Illumination configuration for in-plane electronic speckle pattern interferometry analysis

$$I_1 + I_2 + 2(I_1 I_2)^{1/2} \cos(\Delta\psi) \quad (1)$$

where I_1 and I_2 denote the intensity of the light scattered by each beam alone and $\Delta\psi$ is the phase difference between the corresponding complex amplitudes. Due to the diffuse nature of the scattered light, the term $\Delta\psi$ varies randomly from one pixel to the next and is in part responsible for the speckles in the observed image. Because the camera lens images the surface, the coordinates of the pixels on the sensor are in correspondence with the coordinate *xy* on the object. A new image is captured after a small displacement δ has taken place. The intensities I_1 and I_2 remain approximately constant, but the phase difference changes to $\Delta\psi + \Delta\psi'$, where $\Delta\psi'$ is equal to the product of the wave number $2\pi/\lambda$ (λ is the wavelength of the laser) and the optical path length difference between the illumination beams in the two exposures. Therefore, a digital subtraction of both images determines *N*, where *N* is an integer that represents the fringe order. If the displacement is in the *y*-direction and the beams are in the plane *yz*, Fig. 1(b) shows that the optical path length difference is equal to $\delta(\cos\theta_1 + \cos\theta_2)$. Therefore displacement is given by

$$\delta = \frac{N\lambda}{\cos\theta_1 + \cos\theta_2} \quad (2)$$

Let $\Delta\varepsilon = d\delta/dy$ be the increment of strain between the two images and $\Delta y = dy/dN$ be the fringe separation. Then, with $\theta_1 = \theta_2 = \theta$, it follows from Eq. (2) that

$$\Delta\varepsilon = \frac{\lambda}{2\Delta y \cos\theta} \quad (3)$$

3. Experimental processes

3.1 Engineering materials and test specimens

The specimens are the engineering steel (SM490B). Their chemical composition and the mechanical properties are shown in Tables 1 and 2. They are designed on the basis of ASTM E338-91 and the test area of the specimen is a rectangular cross section, which is 45 mm in width and 14 mm in thickness. The machined notches of V type are made at the middle of both sides using an electric discharge treatment. The geometry of the DENT specimen is shown in Fig. 2 (ASTM 1999).

3.2 Fatigue crack growth test

In this paper fatigue crack growth tests were conducted on the UTM (universal testing machine),

Table 1 Chemical composition of SM490B

Material	Composition (weight %)				
	C	Si	Mn	P	S
SM490B	0.18	0.55	1.60	0.035	0.035

Table 2 Mechanical properties of SM490B

Yield stress (MPa)	325
Ultimate tensile stress (MPa)	490
Young's modulus (MPa)	202,000
Poisson's ratio	0.3

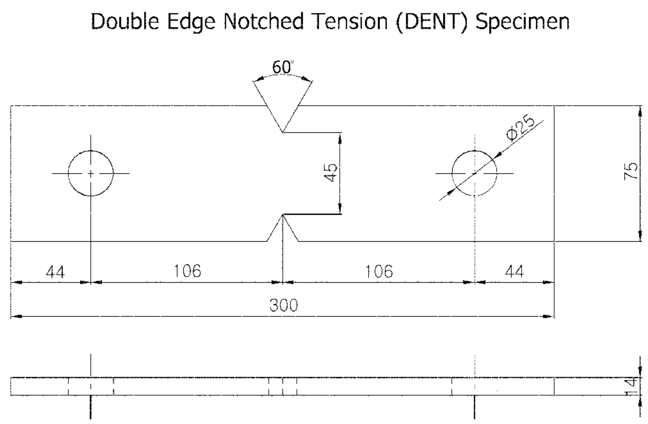

Fig. 2 Geometry of the DENT specimen (unit: mm)

which is taken under load control by a digital computer at room temperature, and using the image analysis system, which is possible to measure for every crack length with the unit of 0.001 mm and travel in x, y and z direction. In the image analysis system, images can be not only transferred from the scope to a computer but also made a database of the images. The fatigue crack growth tests of two types were conducted under constant-amplitude loading with a load ratio $R = 0.2$ and a loading frequency of 3 Hz in a shape of sine wave with a mean load 45 kN and load amplitude 30 kN. The plastic zone size at the crack tip and the crack growth length were measured by ESPI system and the image analysis system.

According to the rules of crack growth test, when a crack growth rate accelerate over 1×10^{-4} mm/cycle, the crack growth rate changes sensitively and its variation increases because of the change of micro structure and crack tip shape like cleavage. Therefore the amplitude of cyclic constant amplitude loading was determined on the basis of crack tip stress intensity factor $\Delta K = 24\ \mathrm{MPa}\sqrt{m}$ in this study. Crack growth rate was made to be in the range of 1×10^{-4} mm/cycle $\sim 1 \times 10^{-5}$ mm/cycle at the time of maximum retardation (ASTM 1999).

4. Test results

4.1 Plastic zone size at the crack tip

In the crack growth test under constant-amplitude loading, the plastic zone size at the crack tip was measured according to the number of cyclic loading using ESPI system to examine the relationship of the plastic zone size and the fatigue crack growth length. When plastic zone appear around crack tip in strain distribution, the shortest distance from the crack tip to the elastic-plastic boundary in crack growth direction is determined in strain contour as the plastic zone size. The change of the strain distribution is shown in Fig. 3 (Kim and Shim 2001).

The plastic zone sizes shown in Table 3 were determined from the strain contour measured by ESPI system. The strain contour was comprised of lines that connect points with the same values of strain in strain distribution. The change of the plastic zone shape is shown in Fig. 4.

For plane strain, the stress σ_z is nonzero, and this elevates the value of σ_x and σ_y necessary to cause yielding, in turn decreasing the plastic zone size relative to that for plane stress. Irwin's estimate of the resulting size is commonly used (Anderson 1995, Dowling 1993).

$$2r_p = \frac{1}{\pi}\left(\frac{K_{\max}}{\sigma_0}\right)^2 \qquad \text{(for plane stress)} \tag{4}$$

$$2r_p = \frac{1}{3\pi}\left(\frac{K_{\max}}{\sigma_0}\right)^2 \qquad \text{(for plane strain)} \tag{5}$$

where $2r_p$, σ_0, $K_{\max}$ are, the plastic zone size, the yield strength and the maximum stress intensity factor.

The plastic zone size equation given is based on simple assumptions and does not consider various complexities which are existed in real structures. However the measured plastic zone size using ESPI system is sufficiently good enough to overcome this problem. The plastic zone sizes on

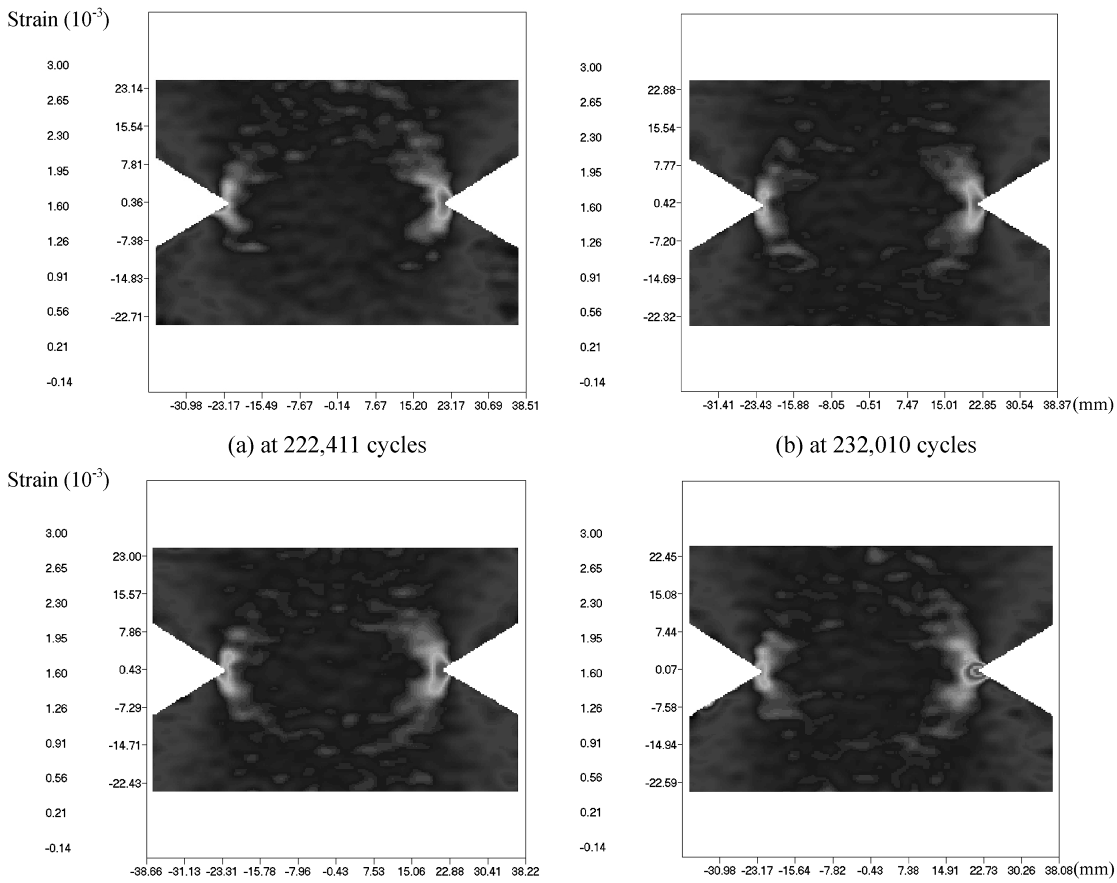

(a) at 222,411 cycles

(b) at 232,010 cycles

(c) at 244,823 cycles

(d) at 267,510 cycles

Fig. 3 Change of strain distribution measured by ESPI system under cyclic loading

Table 3 The plastic zone sizes at the crack tip measured by ESPI system

Cycles	Plastic Zone Size (mm)
281,476	1.00854
299,601	1.15783
308,741	1.16589
317,740	1.24387

specimen surface for the different crack growth lengths are shown in Fig. 5. Longer crack growth length results in larger values of plastic zone size.

Experimental results for plastic zone size at the crack tip using ESPI system are compared with one proposed by Irwin's estimate in Table 4.

Table 4 is a calculated result for plane stress and strain using Irwin's equation according to the crack growth length measured by ESPI system. DENT specimens were not in a state of plane stress

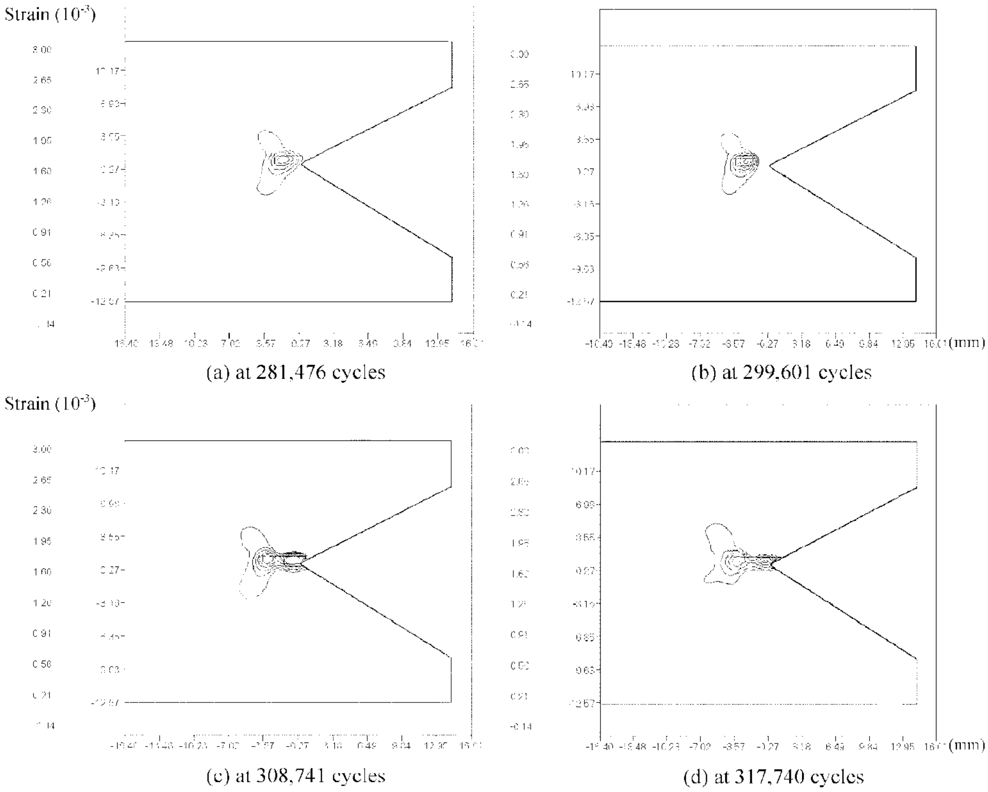

Fig. 4 Change of plastic zone shape on specimen surfaces using ESPI system

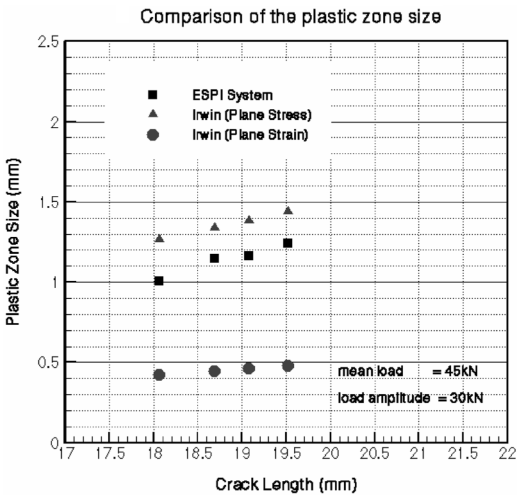

Fig. 5 Comparison of the plastic zone sizes on the basis of the crack length measured by ESPI system

and also plane strain. Therefore, the calculated plastic zone size using ESPI system shown in Fig. 5 is a result considering the effect of thickness of specimen.

Table 4 Calculation of the plastic zone sizes using the crack length measured by ESPI system

Cycles	Crack Length	Plastic Zone Size (mm)		
		ESPI System	Irwin's Equation	
			Plane Stress	Plane Strain
281,476	18.060	1.00854	1.26525	0.42175
299,601	18.690	1.15783	1.33583	0.44528
308,741	19.080	1.16589	1.38210	0.46070
317,740	19.520	1.24387	1.43695	0.47898

Table 5 Comparison of the crack length

	Crack Length	
	ESPI System	Image System
a_{281476} (mm)	18.06	16.036
a_{299601} (mm)	18.69	16.680
a_{308741} (mm)	19.08	17.092
a_{317740} (mm)	19.52	17.549

Note: a_n is the crack growth length at n cycle loading.

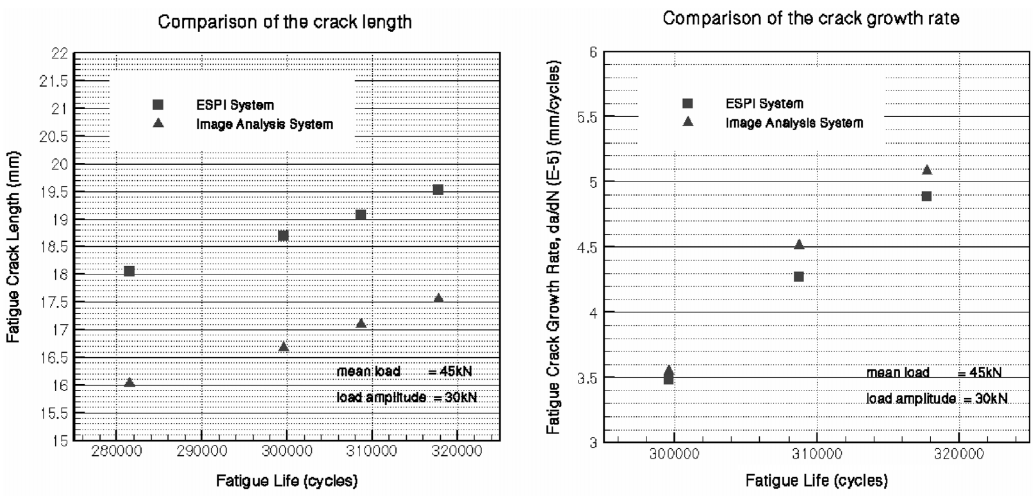

(a) Crack length curve (a) Crack growth rate curve

Fig. 6 Comparison of curves determined by ESPI system and image analysis system

4.2 Fatigue crack growth length

According to the accumulation of fatigue damage, the fatigue crack growth length was measured

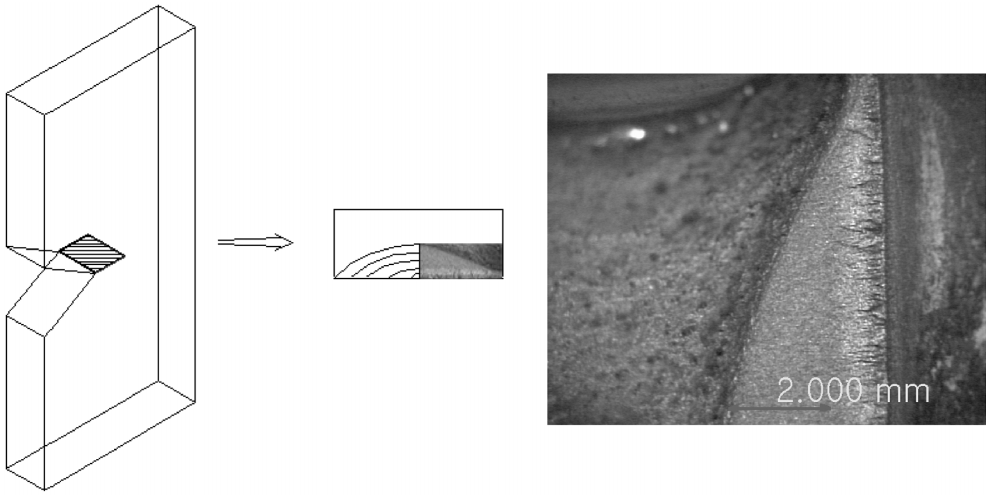

Fig. 7 Image of fracture surface in specimen using image analysis system

by the image analysis system and ESPI system in all fatigue crack growth tests. ESPI system can measure strain distribution in x, y and z direction. The crack growth length is determined from the nonlinear strain gradient in z direction due to crack. Table 5 and Fig. 6 show a comparison of the crack growth length measured by ESPI system and the image analysis system. The results of the inner crack growth length measured by ESPI system and the surface crack growth length measured by image analysis system were compared. There is a constant difference between data. The variance of stress distribution in the thickness direction caused the difference of crack length between inner crack and surface crack (Fig. 7). This comparison showed this difference.

5. Calculation of plastic zone size by FEM

The calculation of plastic zone size in DENT specimen under constant amplitude cyclic loading was carried out using nonlinear static solution in MSC/NASTRAN. Finite element models were used quadratic solid model to model three-dimensional solids. In modeling, the elements that aspect ratio approached under 1.3 were used at crack tip in order to yield best results. The crack length used in finite element analysis is the result measured in crack growth test using ESPI system. For each crack length, crack growth models that two nodes were separated at one location were made along the crack of the finite element model in order to maintain same condition with the crack length in the crack growth test. The plastic zone size was determined as the length from the crack tip to the elastic-plastic boundary in a result of finite element analysis. For each crack length, results calculated by finite element method were compared with them measured by ESPI system in Table 6 and Fig. 9.

According to the crack growth length, the strain distribution around the crack tip was calculated by MSC/NASTRAN. The calculated results are shown in Fig. 8.

The plastic zone shape measured by ESPI system includes the effect of actual material properties and geometries of crack. However the plastic zone shape calculated by FEM can be obtained under

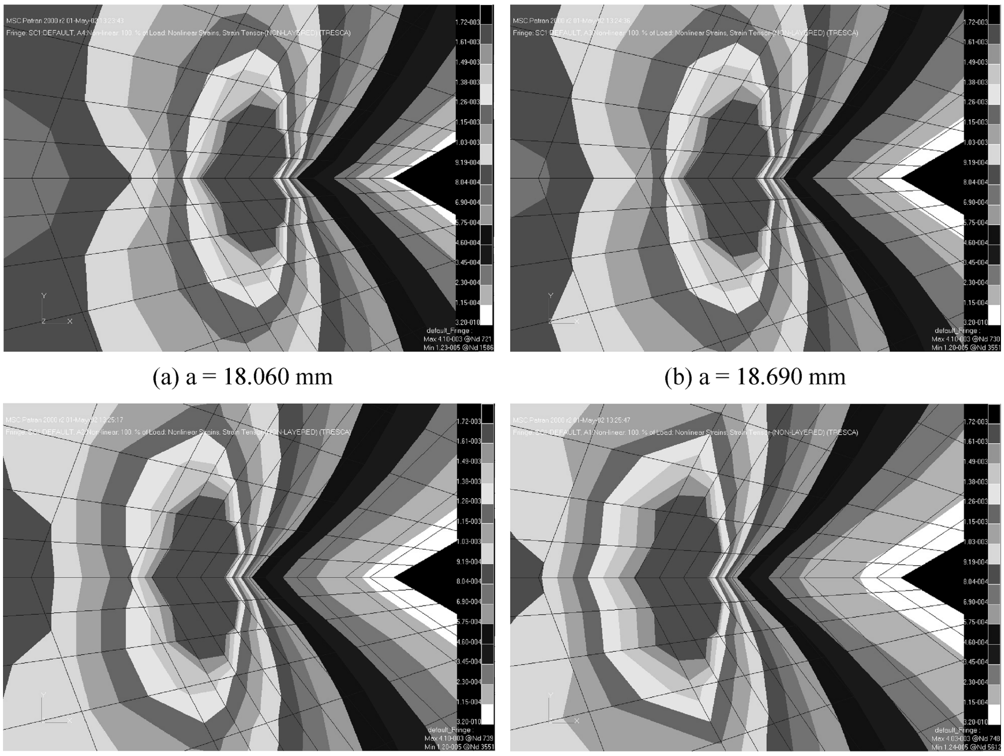

(a) a = 18.060 mm (b) a = 18.690 mm

(c) a = 19.080 mm (d) a = 19.520 mm

Fig. 8 Change of the plastic zone shape according to the crack growth length

Table 6 Calculation of the plastic zone sizes at the crack tip

Cycles	Crack Length	Plastic Zone Size (mm)	
		ESPI System	FEM Analysis
281,476	18.060	1.00854	0.9693
299,601	18.690	1.15783	1.0411
308,741	19.080	1.16589	1.0770
317,740	19.520	1.24387	1.2206

ideal conditions. Although they have some difference in local shape of plastic zone, they are similar in global shape of plastic zone.

6. Conclusions

1) The measured plastic zone sizes are between the values for the plane stress and the plane strain calculated by Irwin's equation as shown in Fig. 5.
2) The results of plastic zone size calculated by elasto-plastic finite element analysis show good

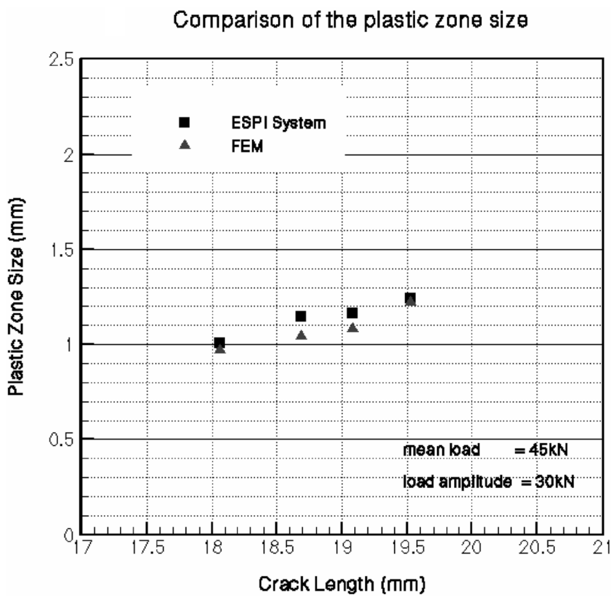

Fig. 9 Comparison of the plastic zone size according to the fatigue crack length

agreement with the measured results by ESPI system within error range of 4~10%.

3) The image analysis system allows the user to measure only the fatigue crack growth length on surface of specimen. However, ESPI system is capable of measuring not only a surface crack length but also an inner fatigue crack growth length.

Consequently, it is confirmed that the ESPI system is appropriate to measure plastic zone size and fatigue crack growth length.

Acknowledgments

This work was partially supported by the Korea Science and Engineering Foundation under Contract 00A-09-02-02-2. The financial support is gratefully acknowledged.

References

Anderson, T.L. (1995), *Fracture Mechanics-Fundamentals and Application*, CRC Press.

ASTM (1999), *Standard Test Method for Measurement of Fatigue Crack Growth Rates*, ASTM Designation E466-96, Annual Book of ASTM Standards, American Society for Testing and Materials, Philadelphia.

Dowling, N.E. (1993), *Mechanical Behavior of Materials*, Prentice-Hall, Inc.

Gong, X.L. and Toyooka, S. (1999), "Investigation of mechanism of plastic deformation process using digital speckle pattern interferometry", *Exp. Mech.*, **39**, 25-29.

Jones, R. and Wykes, C. (1989), *Holographic and Speckle Interferometry*, Cambridge University Press, Cambridge.

Kim, K.S. and Shim, C.S. (2002), "A study on the effect of stress concentration factor determined by 3D-ESPI system on the fatigue life", *J. Ocean Eng. Tech.*, **16**(1), 46-51.

Nam, K.W. (2001), "Life prediction of fatigue crack propagation and nondestructive evaluation in 5083 aluminum alloy", *J. Ocean Eng. Tech.*, **15**(2), 94-98.